2021 International Conference on Unmanned Aircraft Systems (ICUAS)
Athens, Greece. June 15-18, 2021

Collaboration between Multiple UAVs for Fire Detection and Suppression

Andrew Moffatt, Nicholas Turcios, Chase Edwards, Atharva Karnik, David Kim, Andrew Kleinman, Vincent (Hien) Nguyen, Victor Ramos, Earvin Ranario, Tomo Sato, Dzianis Uryeu, and Subodh Bhandari

***Abstract*— This paper presents the use of two UAVs to detect and suppress fires. The first UAV is the detection system and begins the mission by autonomously flying a predetermined route while scanning an area of interest. The UAV is equipped with an infrared sensor for fire detection and a LiDAR for obstacle detection. The fire intensity and fire location information collected by the detection UAV is then relayed to the suppression UAV to start the next phase of the mission. The second UAV features a suppression system capable of suppressing localized fires using a bucket carrying a retardant appropriate for the mission. It will then navigate autonomously to the desired location, and deploy the suppressant. Development of UAV platforms and experimental results including flight test results are shown.**

I. Introduction

Combating uncontrolled and wildfires is essential to protecting property and lives. Wildfires result in the loss of thousands of lives every year and economic losses of hundreds of billions of dollars annually. Accurate and early detection of fires along with predictions of their potential spread is key to the fire management and the safety of firefighters. Thus, there is a need for better and more effective methods to detect, monitor, and suppress wildfires. Traditional methods for remote fire detection and monitoring include ground-based systems and satellite or manned aircraft based remote sensing techniques. Ground-based systems suffer from limited range and may be dangerous to the operation crew. Satellite-based systems can cover large areas, but these systems are very expensive, and resolution is too low to be useful for fire spread estimation and suppression efforts. Manned aircraft-based systems are also expensive, and turnaround time is too long, thereby making them unsuitable for real-time fire monitoring. Moreover, these hazardous environments are too dangerous for pilots and other crew members.

UAV-based remote sensing techniques provide a safe and low-cost alternative for fire detection and suppression. The UAV-based systems provide high resolution data needed for accurate determination of fire location [1, 2]. UAVs can fly repeatedly for long-time and even in the nighttime without putting human resources into danger, and thus providing real-time data round the clock. Most of the tasks can be done automatically as UAVs can be equipped with cheap autopilots for autonomous operation. UAVs can also help reduce the cost associated with fire suppression and detection. This paper explores the use of UAVs and an infrared camera to autonomously locate fires and how that information can be relayed to a second UAV to autonomously suppress the flames. As the UAVs are limited by payload capacities, range, and endurance, using multiple UAVs for fire detection can effectively cover large areas, thereby increasing mission efficiency [3] and reducing or eliminating risks to firefighters. Additionally, large fires can often result in manpower shortages. A fleet of autonomous UAVs can be a future solution for fire detection, monitoring, and suppression.

This paper explores the use of two UAVs, one with an infrared camera to autonomously locate fires, and a second UAV to autonomously suppress the flames using data gathered from the former. In addition, using sense and avoid and path planning techniques, UAVs can also be used for fire detection and suppression in urban and residential areas. This allows UAVs to identify fires outside the view of a ground crew and potentially obscured even to a helicopters.

Subodh Bhandari is a Professor in the Department of Aerospace Engineering at California State Polytechnic University Pomona (phone: 909-869-2612 email: sbhandari@cpp.edu)

Andrew Moffatt is an undergraduate in the Department of Aerospace Engineering at California State Polytechnic University Pomona (email: ajmoffatt@cpp.edu).

Nicholas Turcios is an undergraduate in the Department of Aerospace Engineering at California State Polytechnic University Pomona (email: nturcios@cpp.edu).

Chase Edwards is an undergraduate in the Department of Aerospace Engineering at California State Polytechnic University Pomona (email: chedwards@cpp.edu).

Atharva Karnik is an undergraduate in the Department of Aerospace Engineering at California State Polytechnic University Pomona (email: ahkarnik@cpp.edu).

David Kim is an undergraduate in the Department of Computer Science at California State Polytechnic University Pomona (email: dskim@cpp.edu).

Andrew Kleinman is a graduate in the Department of Computer Science at California State Polytechnic University Pomona (email: akleinman@cpp.edu).

Vincent Nguyen is a graduate in the Department of Computer Science at California State Polytechnic University Pomona (email:hhnguyen@cpp.edu).

Victor Ramos is a graduate in the Department of Electrical and Computer Engineering at California State Polytechnic University Pomona (email: vjramos@cpp.edu).

Earvin Ranario is an undergraduate in the Department of Aerospace Engineering at California State Polytechnic University Pomona (email: ebranario@cpp.edu).

Tomo Sato is an undergraduate in the Department of Aerospace Engineering at California State Polytechnic University Pomona (email: tmsato@cpp.edu).

Dzianis Uryeu is an undergraduate in the Department of Computer Science at California State Polytechnic University Pomona (email: duryue@cpp.edu).

978-0-7381-3115-3/21/$31.00 ©2021 IEEE

The rest of the paper is organized as follows. Section II discusses the hardware components used to support fire detection. Detection of wildfires and their location using an IR sensor is discussed in Section III. Communication between UAVs and autonomy are discussed in the fourth section. Suppression UAV system is presented in Section V followed by conclusion and future work in the last section.

The paper is organized as follows. Section II discusses the hardware components used for both detection and suppression missions. Section III covers flight planning algorithms and simulation. Section IV discusses the methods used for fire detection and determination of fire location. Flight test results are analyzed in Section IV followed by conclusions and future work in the last section.

II. UAV AND FLIGHT HARDARE

A. UAV Platform

The UAV used for this project is the Matrice 600 multicopter, which is shown in Fig. 1. This particular UAV was chosen because of its longer endurance and higher payload capacity. The Matrice 600 has an empty weight of 9.6 kg with the standard battery loaded onto it. It has a maximum takeoff weight of 15.1 kg with a total flight time of 18 mins.

Figure 1. M600 UAV platform

The UAV is equipped with an A3 flight controller from DJI for autonomous waypoint navigation. In addition, the frame of the UAV is easy to modify sensor mounting. Furthermore, the rail system on the undercarriage of the UAV allows for simple integration of a suppression system as seen in Fig. 2.

Figure 2. M600 With Suppression System

B. Onboard Computer

An Intel NUC processor, shown in Fig. 3, is used as a flight computer to process the large volume of information received from the LiDAR and the inertial measurement unit (IMU). It also processes the obstacle avoidance algorithm. It is a small form factor processor featuring a fourth-generation intel processor [4].

Figure 3. Intel NUC processor

D. IR Sensor

The IR sensor that is being used in this project is the FLIR TAU thermal camera shown in Fig. 4. This camera has a 19 mm lens with Field of View (FOV) of $24^{\circ} x\ 18^{\circ}$ and spectral band of 7.5 - 13.5 μm.

Figure 4. FLIR TAU IR camera

The sensor is connected to the onboard computer using an A/D converter for onboard data processing.

E. LiDAR

The Light Detection Ranging (LiDAR) sensor used in this project is the VLP-16 (Puck) LiDAR from Velodyne [4]. The LiDAR, shown in Fig. 5, offers a 360° horizontal and 30° vertical field of view. This greatly enhances detection abilities over traditional one or two dimensional LiDARs. It has a weight of 590 grams and a range of 100 meters with a power requirement of only 8 watts. Its light weight and low power requirements make it very suitable for use with small UAVs. Previously available LiDARs were unsuitable for use with small UAVs because they were either heavier or had a smaller range.

Figure 5. VLP-16 Puck Lite LiDAR

An obstacle avoidance system has been developed, which uses the 360° image generated by the LiDAR [4]. The system finds an obstacle free path before giving the UAV a velocity vector to follow. The LiDAR settings can be accessed directly by connecting to the user interface at IP 192.168.1.201. From this interface, the user can change the RPM to anywhere in between 300 to 1200 RPM. The interface can also change the way the LiDAR collects data, such as changing the FOV and changing the return type.

A 3 cell battery is the power source for the LiDAR. A power analysis was conducted and concluded that the battery has a life of approximately 29 minutes, which is sufficient time for the mission it is used for.

F. Sensor Mounts and Power Distribution

In order for the UAV to detect active fires, all necessary sensors must be carried as the payload during flight. Sensor mounts were designed and selected to carry the payload based on material strength and weight.

Two separate payload fixtures were required: a lower sensor mount carrying the infrared camera, an Intel NUC processor, a lithium-ion rechargeable battery, as well as an upper mount carrying a single VLP-16 LiDAR. The upper mount, shown in Fig. 6, was designed to solely hold the 0.83 kg LiDAR with antenna. Rotor interference was also taken into account. This upper sensor mount consists of a large platform for the LiDAR, and an additional smaller platform over it for the LiDAR console box. The diameter of the circular platform that is holding the LiDAR is 20 cm and the thickness is 1 cm. The top platform is 8 cm tall in relation to the higher platform of the lower base, with a 12 cm x 12 cm plate.

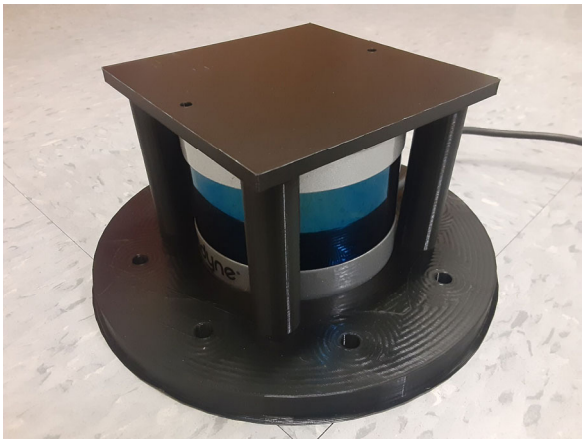

Figure 6. Upper LiDAR mount

The lower sensor mount, shown in Fig. 7, has two separate parts with slots for attachment. This increases the area available for wiring and evenly distributes the center of mass. The front facing section of the lower mount has a slot with an angle of 40° for the infrared camera. This angle gives the camera a higher field of view for flight at lower altitudes. The lower mount total assembly has a length of 31.18 cm and a maximum height of 15.87 cm. The mounting arms have a length of 15.91 cm, allowing plenty of space between the payload and the chassis of the UAV.

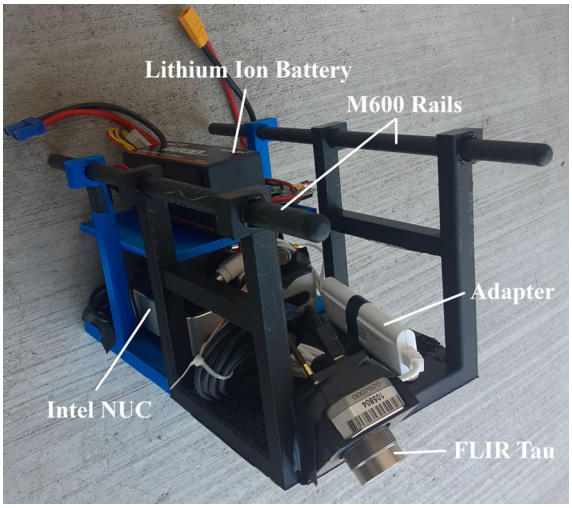

Figure 7. Lower sensor mount assembly

In order to reduce the weight of mounts, the parts were 3D-printed using PLA plastic filaments. Stress analysis was conducted to make sure that the mount would be able to bear the loads during flight without failure.

In addition to the sensor mounts, a power distribution model was designed and integrated with the sensor mount. The same model was functional for both fire detection and fire suppression missions and relied on one 14.8 Volts, 6200mAh LiPo battery. For components requiring different levels of power, appropriate adapters and voltage converters were used to step down the central voltage. Fig. 8 shows the designed power distribution model and how it can be configured for both the detection and suppression missions

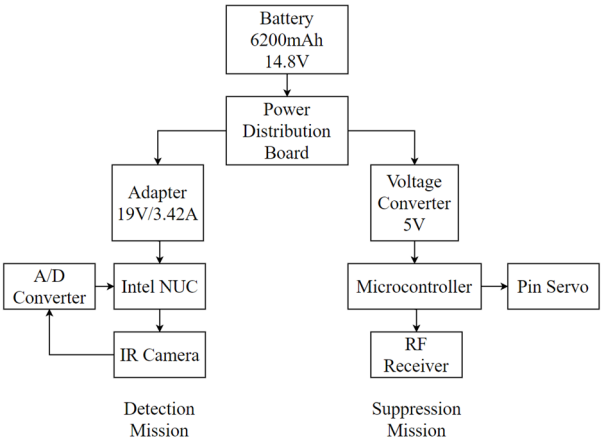

Figure 8. Power distribution schematic.

G. Bucket for Fire Suppression

The fire suppression mechanism includes a bucket for dropping water onto the fire from the UAV. The bucket is made of neoprene, a waterproof, flexible fabric that has been coated with wax. The shape of the bucket is a 5-sided cone that is open at the top and bottom. The fabric is turned inside out to facilitate filling the bucket with water. A cable is then attached to the portion turned inside out and is held by a payload release pin. The fabric bucket is secured to a frame made of delrin, which provides the bucket with its shape and structure as seen in Fig. 9.

Figure 9. Bucket in suppression configuration

The bucket frame is suspended by cables that are attached to a mounting plate on the UAV as shown in Fig. 10. The cables are 5 feet long each. The long cables allow the bucket to be placed on the ground next to the UAV to fill it with water without the risk of being hit by the rotor blades. The mounting plate is a thin piece of delrin with clamps on both sides that secure to the UAV. In the middle, the payload release mechanism is mounted on the underside. Several holes were drilled to create a waffle pattern to reduce the weight of the mounting plate and maximize water capacity.

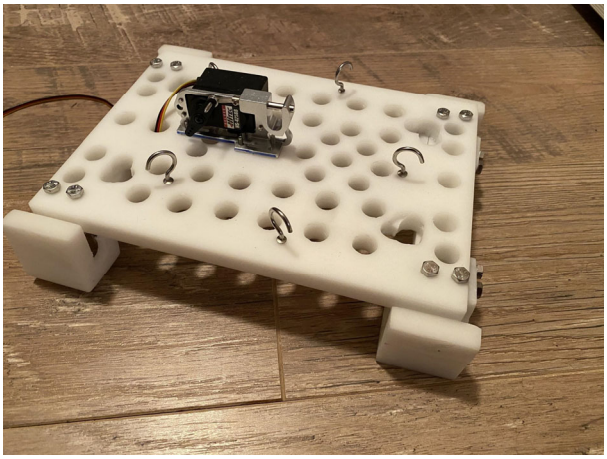

Figure 10: Bucket mounting plate

To release the water from the bucket, the payload release pin is pulled by a servo, as shown in Fig. 10, and the cable holding the fabric inside of itself is then flipped to its natural state as shown in Fig. 11 due to the weight of the water. The Bucket can hold up to 1.2 gallons of water.

Figure 11. Bucket after payload release

H. Microcontroller & RF Module

For the communication and control of the servo for the bucket release mechanism, two Arduino boards were used. The Arduino on the ground station takes commands from the ground station computer, and then sends the command through an APC220 RF Module to the Arduino on board the UAV that sends commands to the dropping mechanism servo.

III. FIRE DETECTION

A. Fire Detection Algorithm

A fire detection algorithm was developed to process the data collected by the thermal camera. The algorithm consists of two main components. The first component preprocesses each frame. The second component determines if a heat source is actually a fire.

The preprocessing starts by applying a Local Intensity operation (LIO) called Intensity brightening operation (IBO). This will cause the image to brighten the bright areas and darken the dark areas [5]. This can be seen in Fig. 12. The equation that is used to apply the IBO is:

$$Z = \prod_{k=0}^{8} z_k \quad (1)$$

where Z is the new pixel calculated by multiplying the surrounded pixel.

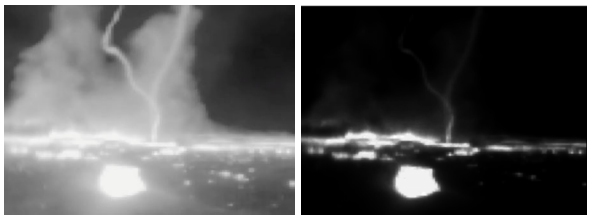

Figure 12. Original Image (left) and IBO image (right)

With the IBO image, shown in Fig. 9 in right, the image is ready to remove the image background and some noise it may have. This results in the image only having the heat sources. This is done by finding the maximum, creating a binary image, and passing the binary image in an area filter as shown in the following equations, respectively [6].

$$gmax = \{(x,y)|\max\{G(x,y)\}\} \quad (2)$$

$$B(x,y) = \begin{cases} 1 \; if \; G(x,y) > \delta_2 * gmax \\ 0 \; if \; G(x,y) < \delta_2 * gmax \end{cases} \quad (3)$$

$$F_k(x,y) = B_k(x,y)|Area(B_k(x,y) > 40 \; \& \; Area(B_k(x,y) > 0.2\alpha \quad (4)$$

In the equations above *gmax* is the max gray level of the image G(x,y) [3]. B(x,y) is the binary image form after using the *gmax* and δ_2 which is the percentage threshold for the fire areas [3]. Lastly $F_k(x,y)$ is the filter image after using the binary image B(x,y) to remove some noise from the fire areas where α is the area of the largest heat source in B(x,y) [3]. After using these equation, resulting images are shown in Fig. 13.

Figure 13. Binary image (left) and image with the area filter (right)

The next major part of the algorithm is to determine if the heat sources found are actual fire sources. This has not been implemented yet. However, the main method that is being investigated uses signatures, wavelet decomposition, and intensity saturation [6]. It may also be possible that fire identification can be achieved by just using signature and intensity [7].

B. Geolocation

After the fire detection, the geo-locations of the hot spots are determined through a real-time direct georeferencing process. Fig. 14 shows all the coordinate frames involved in the calculations.

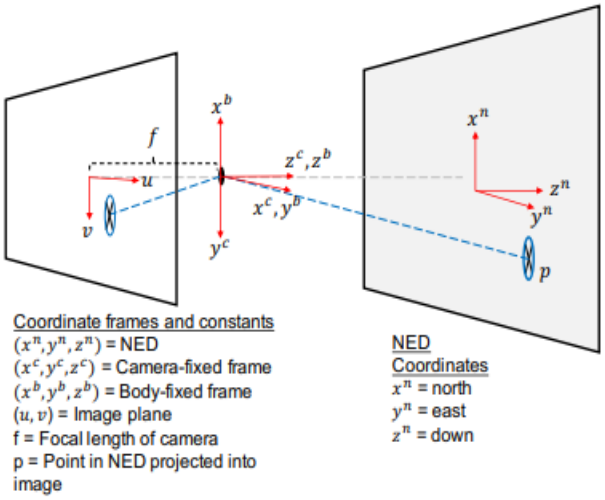

Figure 14. Georeference coordinate frames

The NED coordinates of the hot spots are computed using the following formula:

$$\begin{bmatrix} N \\ E \\ 1 \end{bmatrix} = z^c G_{NE}^{-1} A^{-1} \begin{bmatrix} u \\ v \\ 1 \end{bmatrix} \quad (5)$$

where z^c is the z-coordinate (altitude) in the camera frame and A is the camera intrinsic matrix and is expressed as:

$$A = \begin{bmatrix} f_x & 0 & c_x \\ 0 & f_y & c_y \\ 0 & 0 & 1 \end{bmatrix} \quad (6)$$

where f_x and f_y are the focal lengths (in pixels) in the horizontal and vertical direction, respectively and are identical for square pixels, and c_x and c_y are the principal points and are theoretically in the image center [8]. The u and v in the equation are the pixel positions of the hot spots obtained from the previous section, G_{NE} is the North-East transformation matrix and is computed using the Euler angles (roll, pitch, yaw) of the body frame and the pan and tilt angles of the gimbal [8]. It is expressed as:

$$G_{NE} = [r_1, r_2, -R_n^c r_{nc}^n] \quad (7)$$

where R_{n^c} is the rotation matrix from NED frame to camera frame,. r_1 and r_2 are the first two column vectors in R_{n^c}, and r_{nc^n} is the position of the origin of the camera frame relative to the NED frame. R_{n^c} is calculated using the equation:

$$R_n^c = (R_b^n R_c^b)^{-1} = (R_b^n (R_m^c R_b^m)^{-1})^{-1} \quad (8)$$

where R_{b^n} is the rotation matrix from body frame to NED frame and is expressed as:

$$R_b^n = \begin{bmatrix} c\psi c\theta & -s\psi c\phi + c\psi s\theta s\phi & s\psi s\phi + c\psi c\phi s\theta \\ s\psi c\theta & c\psi c\phi + s\phi s\theta s\psi & -c\psi s\phi + s\theta s\psi c\phi \\ -s\theta & c\theta s\phi & c\theta c\phi \end{bmatrix} \quad (9)$$

where ϕ, θ, and Ψ are the roll, pitch, yaw angles of the body frame, respectively, and $c\theta = \cos(\theta)$ and $s\theta = \sin(\theta)$. R_m^c is the rotation matrix from gimbal frame to camera frame and is expressed as:

$$R_m^c = \begin{bmatrix} c\psi_g c\theta_g & s\psi_g c\theta_g & -s\theta_g \\ -s\psi_g & c\psi_g & 0 \\ c\psi_g s\theta_g & c\psi_g s\theta_g & c\theta_g \end{bmatrix} \quad (10)$$

where Ψ_g and θ_g are the pan and tilt angles of the gimbal in case the camera is mounted in a gimbal [8]. If the camera is attached directly to the airframe, R_m^c is the identity matrix.

The overall complexity of this georeference algorithm is dependent on the complexity of obtaining the pixel positions of hot spots using object detection's algorithm in step 1 [8].

Finally, the position of the fire is relayed back to the suppression UAV in the form of GPS position coordinates.

The FLIR Tau thermal camera has a feature called Isotherms, which adds color when a pixel is in a certain thermal range. As a result, this feature was used to help identify if a fire is in a frame. Furthermore, the setting for this feature was set as follows: Upper - 95% and Lower - 90%. These settings produced the image shown in Fig. 15 (left). Furthermore, with a simple color detection algorithm that isolated the red color in Fig.15 on the left produced the figure in the right.

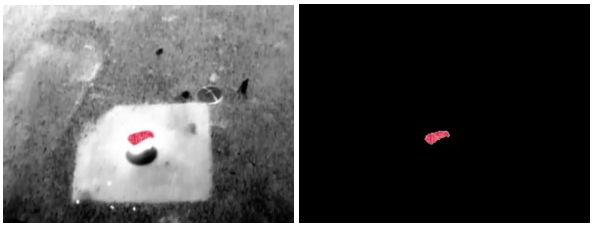

Figure 14. Fire in image highlighted (left) and fire in image isolated (right)

IV. FLIGHT PLANNING

A. Dronekit and Simulation

To allow the detection UAV to navigate in a hazardous environment, a flight control software must be used. DroneKit is an open-source library that was used to create applications for UAVs by connecting the onboard companion computer to the flight controller over MAVLink, which is a lightweight messaging protocol that uses a hybrid publish-subscribe and point-to-point design pattern. This provides the telemetry as well as the state and parameter information to the companion computer to control the UAV actions and movements [1, 6]

DroneKit-SITL (Software in the Loop) simulation allows for testing applications on a virtual UAV by connecting to a virtual environment and ground station application such as APMPlanner through the User Datagram Protocol (UDP). By using SITL simulation, algorithms and applications can be tested prior to flight without the risk of damaging the UAVs and equipment onboard. This allows for simulating a UAV flight before flight test, decreasing costs, and increasing the odds of a successful flight in a production environment. After a successful flight in a simulation, applications would then be implemented into the companion computer for real flight.

However, this flight control software currently only works for Pixhawk flight controllers. Integrating this algorithm with DJI's A3 software development kits will be done in future.

B. Path Planning Algorithm

The primary path planning algorithm implemented on the detection UAV uses an "edge detection" method [4]. Fig. 16 shows how the edge detection method works. As seen, when an obstacle is found, the algorithm alternate obstacle free path.

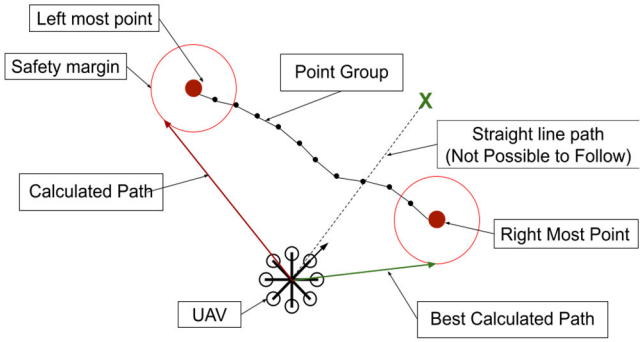

Figure 16. UAV trajectory when encountering an obstacle

An additional obstacle avoidance algorithm will be running at more frequent intervals to detect obstacles when the UAV is on a collision course. This algorithm serves to scan for moving obstacles and changes within the environment in a time-efficient manner, to limit strain on the onboard computer while constantly maintaining obstacle avoidance capabilities.

This algorithm first checks if the LiDAR data includes any points within the general direction and magnitude of the UAV's current velocity. If none are found, there is no obstacle nearby, and the avoidance algorithm does not continue. If an obstacle is found nearby, another method will determine if there is a direct collision course with the UAV and a margin around its current path. If there is, the algorithm will communicate a change of velocity to the Dronekit, and initiate a brief delay before the edge detection algorithm can be run again. This delay does not affect the obstacle avoidance subsystem, and provides sufficient time to move to a safe distance away from nearby obstacles.

V. TEST RESULTS

A. Fire Detection UAV Testing

The Detection UAV has been tested in manual flight to collect data from the infrared camera as shown in Fig. 17.

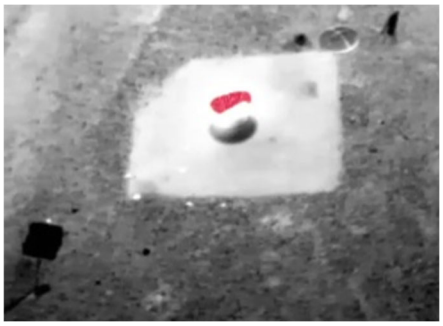

Figure 17. Detection flight test IR image

The fire detection algorithm successfully determined the presence of a fire during a simulated mission. The image was captured roughly at a height of 13 meters with the camera positioned at a 40 degree angle. Fig. 18 shows the position of the fire relative to the camera during the flight test.

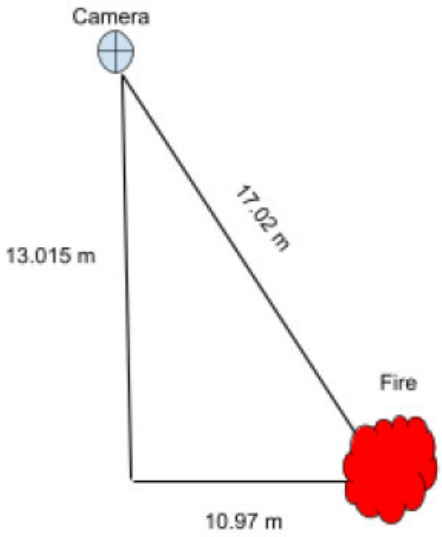

Figure 18. Camera-fire-takeoff point triangle

According to the pinhole camera model, given the 2D coordinate of the fire in the processed thermal image and camera specifications, distance between the camera and the fire can be determined. From there, the NED coordinates of the fire is calculated and then transformed to Geodetic (GPS) coordinates for suppression UAV. Table 1 shows the determined calculated and actual distances between the UAV and fire as well as the GPS coordinates of the fire.

Table 1. CALCULATED AND ACTUAL COORDINATES OF FIRE

	Calculated	Actual	Error
Distance (m)	21.82	17.02	28.20%
Latitude (°)	33.9321	33.9319	-
Longitude (°)	-117.6311	-117.6311	-
Altitude (m)	166	166	-

The largest source of error comes from the latitude calculated. If this was an autonomous mission, the Suppression UAV would miss the fire by about 3 meters. However, in a larger fire, this tolerance would be more acceptable as there would be more data available to more accurately determine the fire locations. Currently, work is underway to improve the detection accuracy.

B. Suppression UAV

Suppression UAV was also tested in manual flight mission. The UAV was successfully able to extinguish a 5 ft^2 fire with 1.2 gallons of water as seen in Fig. 19.

Figure 19. Suppression UAV flight test showing water drop

VI. CONCLUSION, TESTS, AND FUTURE WORK

This paper presented the collaboration between UAVs for coordinated fire detection and suppression mission. The location of the identified fire using an IR sensor aboard the Detection UAV was sent to the Suppression UAV, which was then navigated to the area of interest to deploy suppressant on the fire. The detection algorithm and suppressant release mechanism have been tested both on ground and during flight.

Additional tests performed include both a structural integrity test and suppressant deployment test for the bucket mechanism as well as multiple verification tests for the fire detection algorithm.

Future work will involve verification of the obstacle avoidance algorithms in simulations using DJI software development kits and additional testing to improve detection accuracy. Future work will also involve using the LiDAR for 3-D mapping of the environment to improve the situational awareness of first responders. Future work will also involve adding more UAVs to the collaborative team of vehicles and using a swarm of vehicles for effective detection and suppression of wildfires using UAVs. Vehicle swarms could also be used to test using multiple suppression UAVs to collectively tackle larger fires with minimal human effort. Finally, increasing the processing speed of the onboard computer will allow for live analysis and make the feed between the detection and suppression drone live.

ACKNOWLEDGEMENTS

The authors would like to acknowledge and thank the funding support provided by the Lockheed Martin Corporation (LMC) that made this work possible. Furthermore, the authors would also like to thank the LMC engineers for providing valuable comments and insight during project reviews.

REFERENCES

[1] V. G. Ambrosia and E. Hinkley, "NASA Science Serving Society: Improving Capabilities for Fire Characterization to Effect Reduction in Disaster Losses," *IEEE International Geosciences and Remote Sensing Symposium*, Boston, MA, July 7-11, 2008.

[2] C. Yuan, Z. Liu, and Y. Zhang, "Fire Detection using Infrared Images for UAV-based Forest Fire Surveillance," *2017 International Conference on Unmanned Aircraft Systems*, Miami, FL, June 13-16, 2017.

[3] S. Bhandari, D. Tang, S. Boskovich, Z. Aliyazicouglu, R. Demonteverde, et al., "Collaboration between Multiple Unmanned Vehicles for Increased Mission Efficiency," *Proceedings of AIAA Infotech@Aerospace Conference, San Diego, CA, January 4-8, 2016.*

[4] A. Moffatt, E. Platt, B. Mondragon, A. Kwok, D. Uryeu, and Dr S. Bhandari, "Obstacle Detection and Avoidance System for UAS using a LiDAR," *Proceedings of the International Conference on Unmanned Aircraft Systems*, Hybrid Event, Athens, Greece, Sept 1-4, 2020.

[5] R. Heriansyah and S.A.R. Abu-Bakar, "Defect Detection in Thermal Image for Nondestructive Evaluation of Petrochemical Equipment," *NDT & E International,* Vol 42, No. 8, pp. 729-740, 2009.

[6] M. Chacon and F. Perez-Vargas, "Thermal Video Analysis for Fire Detection Using Shape Regularity and Intensity Saturation Features," *Third Mexican Conference in Pattern Recognition*, Cancun, Mexico, June 29-July 2, 2011.

[7] I. Bosch, S. Gomez, R. Molina and R Miralles "Object Discrimination by Infrared Image Processing," *Bioinspired Applications in Artificial and Natural Computation, Third International Work-Conference on the Interplay Between Natural and Artificial Computation*, Santiago de Compostela, Spain, June 22-26, 2009.

[8] H. Helgesen, F. Leira, T. Bryne, S. Albrektsen, T. Johansen, "Real-Time Georeferencing of Thermal Images Using Small Fixed-Wing UAVs in Maritime Environments," *ISPRS Journal of Photogrammetry and Remote Sensing*, Vol 154, pp. 84-97, 2019.